

## Sediment dispersal and accumulation off the Ayeyarwady delta – Tectonic and oceanographic controls



Steven A. Kuehl<sup>a,\*</sup>, Joshua Williams<sup>a</sup>, J. Paul Liu<sup>b</sup>, Courtney Harris<sup>a</sup>, Day Wa Aung<sup>c</sup>, Danielle Tarpley<sup>a</sup>, Mary Goodwyn<sup>a</sup>, Yin Yin Aye<sup>d</sup>

<sup>a</sup> Virginia Institute of Marine Science, Gloucester Point, VA, USA

<sup>b</sup> North Carolina State University, Raleigh, NC, USA

<sup>c</sup> University of Yangon, Yangon, Myanmar

<sup>d</sup> Mawlamyine University, Mawlamyine, Myanmar

### ARTICLE INFO

Editor: Edward Anthony

### ABSTRACT

Recent sediment dispersal and accumulation on the Northern Andaman Sea continental shelf, off the Ayeyarwady (Irrawaddy) and Thanlwin (Salween) Rivers, are investigated using seabed, water column, and high-resolution seismic data collected in December 2017.  $^{210}\text{Pb}$  and  $^{137}\text{Cs}$  derived sediment accumulation rates are highest (up to  $10 \text{ cm y}^{-1}$ ) in the mid-shelf region of the Martaban Depression, a basin that has formed on the eastern side of the N-S trending Sagaing fault, where rapid progradation of a muddy subaqueous delta is occurring. Landward of the zone of highest accumulation, in the shallow Gulf of Martaban, is a highly turbid zone where the seabed is frequently mixed to depths of  $\sim 1 \text{ m}$  below the sediment water interface. Frequent resuspension in this area may contribute to the formation of extensive fluid muds in the water column, and consequent re-oxidation of the shallow seabed likely reduces the carbon burial efficiency for an area where the rivers are supplying large amounts of terrestrial carbon to the ocean. Sediment cores from the Gulf of Martaban have a distinctive reddish brown coloration, while x-radiographs show sedimentary structures of fine silt laminations in mud deposits, which indicates strong tidal influences. The seaward part of the Martaban Depression off the modern subaqueous delta is covered by relict sediment, with no apparent connection between the modern sediment deposit and the offshore Martaban canyon. On the western side of the Sagaing fault, the "Mouths of the Ayeyarwady" represent a large promontory where the subaerial delta has prograded seaward some  $\sim 200 \text{ km}$  along the eastern flank of the Indo-Burman range since the Holocene maximum transgression. The shelf area off the "Mouths of the Ayeyarwady" presently exhibits low sediment accumulation rates ( $\sim 1 \text{ cm y}^{-1}$ ) and a relative coarse (sandy) texture. The reduced accumulation and coarse texture in the western shelf region at the present time is attributed to frequent wave resuspension, and subsequent transport of finer river-derived sediment eastward (into the Martaban Depression) during the SW Monsoon. A mud drape (accumulation rates  $< 1 \text{ cm/yr}$ ) is present on the northwestern part of the delta, where some sediment likely escapes the shelf to the deeper Bay of Bengal. In contrast with the Gulf of Martaban, sediments in this mud drape show olive grey coloration, while sedimentary structures are dominated by mottled sandy mud with shells, and occasional sand layers. The mud drape is likely derived from a mixture of local rivers draining westward from the Indo-Burman range, and a contribution from the Ayeyarwady system delivered during the NE monsoon. Overall, the shelf offshore the Ayeyarwady and Thanlwin rivers represents a compound subaqueous delta with marked differences from east to west that are controlled by a combination of oceanographic and tectonic factors.

### 1. Introduction

The world's rivers collectively discharge about  $36,000 \text{ km}^3$  of freshwater and  $> 20$  billion tons of solid and dissolved material to the global ocean annually (Milliman and Meade, 1983; Milliman and

Syvitski, 1992; Milliman and Farnsworth, 2011), and are a dominant control on the physical and biogeochemical features of continental margins (McKee et al., 2004; Meybeck et al., 2003; Bianchi and Allison, 2009). River deltas forming at the mouths of many of the larger rivers are densely populated, house megacities (e.g., Bangkok, Shanghai,

\* Corresponding author.

E-mail address: [kuehl@vims.edu](mailto:kuehl@vims.edu) (S.A. Kuehl).

Dhaka) and support expansive agriculture and mariculture (Svitski and Saito, 2007). The 25 largest rivers of the world drain approximately half of the continental surface and transport about 50% of the fresh water and 40% of the particulate matter entering the ocean (Bianchi et al., 2013). Under present high sea-level conditions, the continental shelf seaward of the mouths of many of these major rivers is a major repository for the sediment delivered there (Korus and Fielding, 2015). Only in a few large river systems are land-derived fluvial sediments able to escape into deep-ocean basins via cross-shelf valleys or submarine canyons (e.g., Ganges-Brahmaputra (Kuehl et al., 1989, 1997), Congo (Savoye et al., 2009), Indus (Clift et al., 2014) and Mississippi (Ross et al., 2009)).

Many of these large deltas face severe pressure from urbanization, land-use changes, socio-economic transformation, climate change, and episodic natural hazards. At present, sediment fluxes in many of the world's large rivers have been reduced sharply due to human activities (Svitski et al., 2009). With increasing anthropogenic influence, 85% of the large deltas are experiencing increased severe flooding, and the delta surface area vulnerable to inundation is predicted to increase by 50% under the current projected values for sea-level rise in the twenty-first century (Svitski et al., 2009; Svitski and Saito, 2007).

Large rivers in Asia are sourced from the Tibetan plateau (Asia Water Tower) that spawns the 7 giant river systems which together "feed" half the population of the world (Fig. 1). Four of these rivers have extensive river control structures (Yangtze, Yellow, Indus, Mekong) that have reduced the sediment flux to the ocean by as much as an order of magnitude (e.g., Gupta et al., 2012). Of the remaining systems (Ganges-Brahmaputra, Ayeyarwady (Irrawaddy), Thanlwin (Salween)), the Ayeyarwady and the Thanlwin are presently considered the last remaining long free-flowing large rivers in Asia outside of the arctic (Grill et al., 2019). The combined Ayeyarwady-Thanlwin currently ranks as the third largest river system in the world in terms of suspended sediment discharge, contributing > 600 MT of sediment annually (Furuichi et al., 2009; Robinson et al., 2007). This system also transports 5.7–8.8 MT  $y^{-1}$  of organic carbon, suggesting that it may be the second largest point source of organic carbon to the global ocean after the Amazon (Bird et al., 2008; Ramaswamy et al., 2008). Despite the global importance of this system, previously very little was known regarding the fate of Ayeyarwady-Thanlwin river-derived sediment on the adjacent shelf (c.f., Rao et al., 2005, Ramaswamy et al., 2004).

## 2. Background

### 2.1. Geologic setting

Both the Ayeyarwady and Thanlwin rivers rise in the eastern Himalayas and flow southward through the center of Myanmar. They discharge within 150 km of each other into the northern Andaman Sea. The catchment rocks of the Ayeyarwady reflect a wide range of ages and lithologies, including, for example: Cretaceous-Cenozoic flysch of the Indo-Burman-Arakan mountain ranges, Eocene-Miocene-Quaternary sediments of the Myanmar Central Basin, and Neoproterozoic and Cretaceous-Eocene metamorphic/basic/ultrabasic rocks of the eastern syntaxis of the Himalayas (Mitchell et al., 2012; Awasthi et al., 2014; Robinson et al., 2014; Garzanti et al., 2016). The Thanlwin rises from glaciers of the Tangula Mountains on the Tibetan Plateau, flowing southwards through Yunnan Province of China, and the Kayan and Mon States of Myanmar (Chapman et al., 2015). The rocks within the drainage basin of the Thanlwin include the magmatic belt of the northern Lhasa block, and Precambrian to Tertiary sedimentary, igneous and metamorphic rocks of the Shan Plateau/Sibumasu block (Mitchell et al., 2012; Awasthi et al., 2014; Robinson et al., 2014). Thus these two rivers, although they parallel each other for most of their lengths, drain geologically distinct catchments.

Major tectonic features controlling the present configuration of the Myanmar region include collision between the Indian and Eurasian

plates, coupling and decoupling of platelets, crustal movement along the fault lines, rotation of continental blocks and opening of marginal basins (Fig. 1) (Khan and Chakraborty, 2005). In this area, the India plate begins its descent into Earth's mantle in the west, and forms a deep N-S striking Andaman trench. On the continental plate, a major fault system extends from south to north: the Sumatra fault and Western Andaman Fault, and further extends to the east and north to form the Sagaing fault (Fig. 1). The Sagaing Fault links two very different, but equally active tectonic domains: the Andaman Sea in the south and the eastern Himalayan syntaxis in the north (Searle and Morley, 2011). The Andaman Sea is an oceanic pull-apart basin lying above and behind the Andaman subduction zone where convergence between the overriding Southeast Asian plate and the subducting Indian plate is highly oblique (Curry, 2005). Like the San Andreas Fault, the Sagaing Fault is an active right-lateral strike-slip fault, and moves at an average of 18–20 mm each year (Vigny et al., 2003).

The northern Andaman Sea continental shelf is part of the complex geological setting of this collision margin (Curry et al., 1979; Curry, 2005). The Sagaing strike slip fault runs through the Gulf of Martaban and the adjacent shelf, extending southward to join the Central Andaman Rift (Curry et al., 1979). The shelf shows sharp contrasts in morphology to the west and east of this fault location. To the east of the fault, the shelf displays a distinctive bathymetric low (Martaban Depression), with water depths > 100 m from the mid shelf seaward to the shelf break (Figs. 1, 2). Martaban Canyon, within this bathymetric low, appears to be controlled by this N-S trending fault system (Ramaswamy and Rao, 2014). The western shelf, in contrast, shows a characteristic ramp morphology, with water depths decreasing gradually toward the shelf break.

### 2.2. Ayeyarwady and Thanlwin Rivers

The Ayeyarwady River is ~2170 km long and has drainage basin area of 413,000 km<sup>2</sup>, with its delta hosting the majority of the 47 million people of Myanmar. The Ayeyarwady enters the Andaman Sea from the western promontory, with several (~10) major distributaries interconnected by innumerable smaller rivers and streams. The Thanlwin River stretches ~2400 km from the Tibetan plateau in China, through Myanmar to the Andaman Sea. The Thanlwin enters the ocean along the eastern side of the delta near the city of Mawlamyine, as a single thread stream.

The Ayeyarwady-Thanlwin delta spans at least 300 km from east to west, and 200 km north to south. Myanmar's largest city, Yangon, is positioned on the eastern side of the delta. The delta lies in the lowest expanse of land in Myanmar and fans out from the limit of tidal influence at Myan Aung to the Andaman Sea, with as much as 200 km of progradation since the Holocene maximum transgression (Giosan et al., 2018). The rich alluvial soil supports cultivation of rice, and a dense population. However, with > 1100 km<sup>2</sup> of land having elevations < 2 m above sea level, and relative sea level rise at least twice the rate of aggradation, the Ayeyarwady delta has been classified as being in peril (Svitski et al., 2009). On May 2, 2008, Cyclone Nargis devastated the densely populated Ayeyarwady delta. With 200 km  $h^{-1}$  winds and torrential rain; it sent a storm surge 40 km inland, caused catastrophic destruction along with massive shoreline erosion and at least 138,000 fatalities, and left about 2.5 million homeless (Fritz et al., 2009; Basset et al., 2017).

### 2.3. Coastal hydrodynamic setting and monsoonal climate

Tides in the northern Andaman Sea are semi-diurnal with M2 (principal lunar) and S2 (principal solar) being the major components. Near the "Mouths of the Ayeyarwady", tidal range is between 2 and 4 m and can be classified as meso-tidal. To the east of the Ayeyarwady promontory, however, the Gulf of Martaban is macrotidal, with a tidal range of nearly 7 m recorded at Elephant Point. During spring tides,

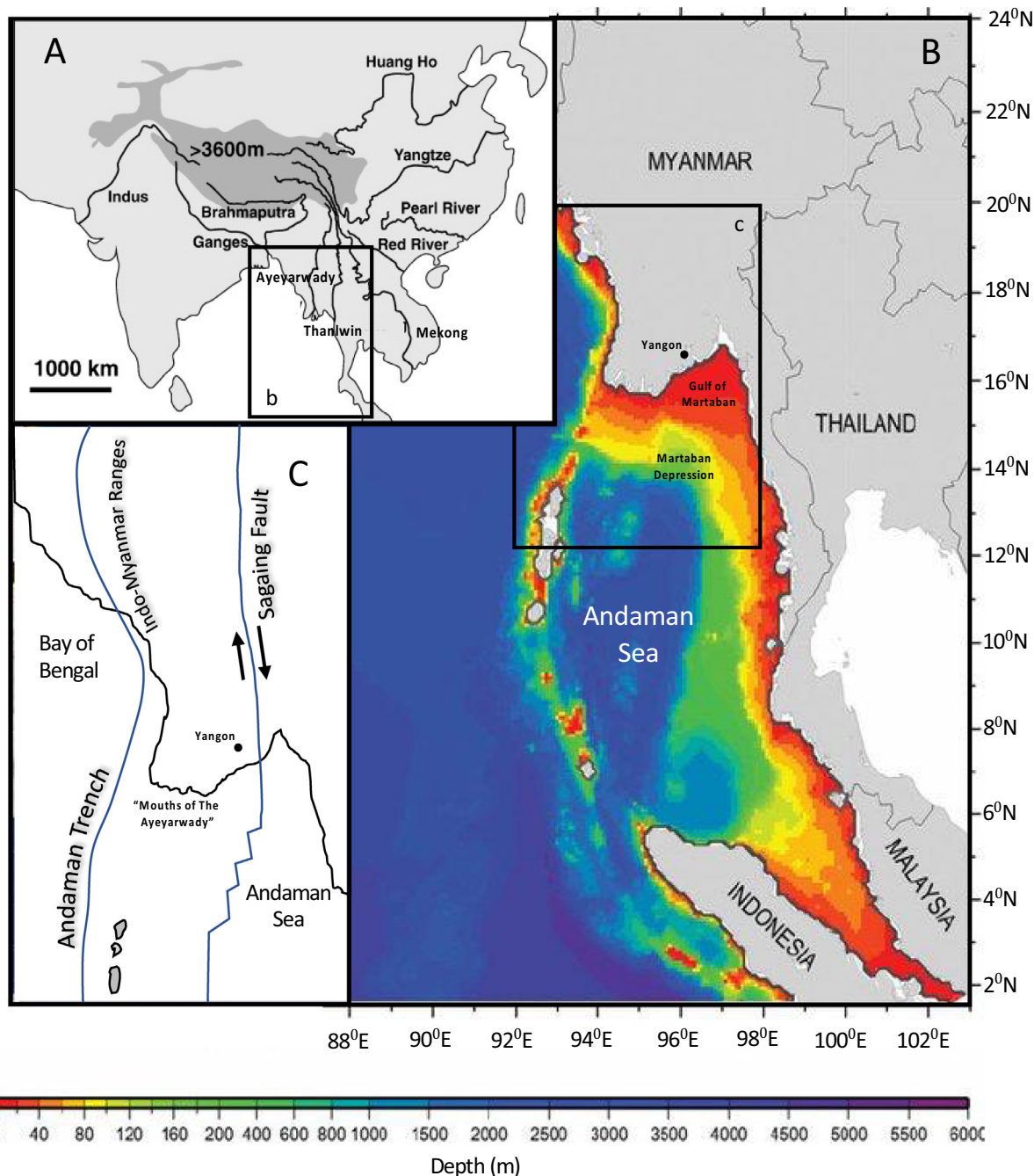


**Fig. 1.** Location maps for study area: (A) Asia map showing major rivers, including the Ayeyarwady and Thanlwin; (B) Andaman Sea bathymetry (after Sindhu et al., 2007); (C) simplified tectonic setting of northern Andaman Sea.

tidal currents reach as high as  $3 \text{ m s}^{-1}$  in the Gulf of Martaban (Rao et al., 2005).

The entire northern Indian Ocean including the Andaman Sea is strongly influenced by the seasonally reversing Asian monsoon (Wyrtki, 1973). The SW monsoon, active between mid-May and October, is accompanied by high precipitation and high river discharge. In contrast, the low-discharge dry season extends from mid-October to mid-May, including the NE monsoon season between December and February (Ramaswamy et al., 2008). In response to the monsoons, currents in the Andaman Sea change direction twice a year with cyclonic flow in spring and summer, and anti-cyclonic flow for the rest of the year (Potemra et al., 1991). Circulation in the Andaman Sea is therefore cyclonic during the SW monsoon (May–September), and anti-cyclonic during the NE monsoon (December–February), but little is known about how this

impacts currents within the Gulf of Martaban region, particularly the bottom boundary layer currents which impact sediment fluxes.

#### 2.4. Sediment dynamics and shelf sediments

Knowledge of sediment transport off the Ayeyarwady-Thanlywin Rivers is limited. Ramaswamy et al. (2004) obtained water samples from > 140 locations along the shelf and shelf/slope break during late springtime, and found that near-bed sediment concentrations were as high 300 mg/l, while the overlying surface water had concentrations of about 10–50 mg/l. Satellite data show that surface suspended sediment concentrations respond strongly to tides, with extensive areas (> 40,000 km<sup>2</sup>) of high surface turbidity (especially in the Gulf of Martaban) during spring tide (Ramaswamy et al., 2004). Furthermore,

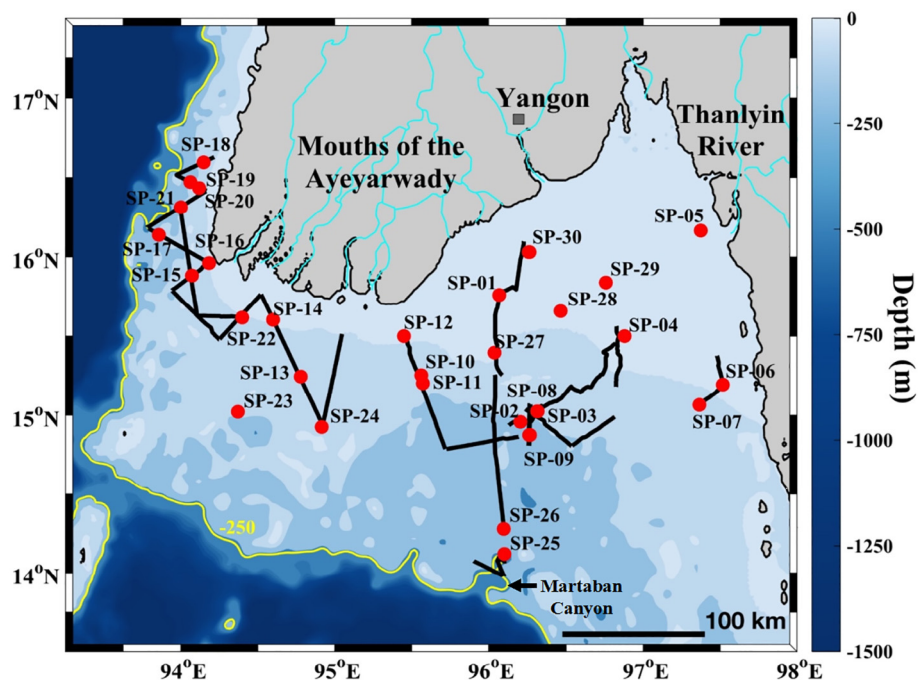


**Fig. 2.** Study area showing coring locations (red circles) and Chirp track lines (black lines) occupied during December 2017. (For interpretation of the references to color in this figure legend, the reader is referred to the web version of this article.)

a decadal record of satellite data repeatedly showed a greater extent of high suspended sediment centration (SSC) in surface waters during the (dry) NE winter monsoon (i.e., from December to January when the surface turbid zone can reach the latitude of  $15^{\circ}\text{N}$ ). In contrast, during the SW monsoon (May–Sept) low and sparse SSC cover area was observed, though this is the time of high discharge (Matamin et al., 2015). The seasonal signal described by Matamin et al. (2015) could result as winds shift from downwelling (SW summer monsoon) to upwelling favorable (NW winter monsoon), though at present we lack observational data to support this idea.

Based on 120 surficial sediment samples collected in April–May 2002, grain-size distribution on the shelf reveals three distinct areas in term of sediment texture: (i) an extensive mud belt in the Gulf of Martaban and adjacent shelf; (ii) outer shelf relict sands; and (iii) locally mixed sediments with relict sands and modern mud (Rao et al., 2005). Geochemical studies of surficial sediments found higher total organic carbon (TOC) and total nitrogen (TN) in the inner-shelf mud belt and on the continental slope sediments, whereas the outer-shelf sediments (possibly relict sands) were low in TOC (Ramaswamy et al., 2008).

From both grain-size and analysis of sparse oceanographic data, it appears that most of the suspended sediment discharge of the Ayeyarwady is transported eastwards to the Gulf of Martaban, contributing to an extensive mud belt there that covers an area of  $> 45,000 \text{ km}^2$  (Rao et al., 2005; Ramaswamy and Rao, 2014). This eastward transport is believed to result from the combination of strong residual tidal currents and clockwise flowing SW monsoon current. Rao et al. (2005) speculated that some suspended sediment discharge reaches the deep Andaman Sea via the Martaban Canyon, and that during winter, counter-clockwise flowing NE monsoon currents transport some sediment westward into the Bay of Bengal.

### 3. Methods

#### 3.1. Wave climate

The global Wave Watch III® model (Tolman et al., 2002) provided hindcast wave properties (significant wave height, mean wave period,

wave direction) at a spatial resolution of  $0.5^{\circ}$ , and temporal resolution of 3 h. The archived model estimates from 2015–present are available from the NOAA National Centers for Environmental Information. To explore seasonal and spatial characteristics in wave processes important for sediment resuspension, we analyzed the Wave Watch III® data for January and August 2016, to characterize wave conditions during the NE and SW monsoon periods, respectively.

#### 3.2. Field data collection

Seabed, high-resolution seismic, and water column data were acquired from the study area using a local vessel out of Yangon (*Sea Princess*) during December 2017. A CTD (RBR XRX-620) package (along with an Optical Backscatter Sensor, OBS, for turbidity) was manually deployed at 10 stations on the shelf and 5 stations in the Yangon River estuary, sampling at 6 Hz during descent through the water column at a rate of  $\sim 20 \text{ cm s}^{-1}$ . These provided water column profile observations of conductivity, temperature, and turbidity. Though conductivity typically is interpreted to represent salinity, previous studies have shown that high levels of turbidity can lower conductivity readings (Held et al., 2014). Therefore, low conductivity readings may indicate either low salinity or high suspended sediment concentrations. An OBS was mounted on the CTD and its voltage readings indicate relative turbidity, but were not calibrated to provide suspended sediment concentration.

Sediment Cores were collected at 30 stations using a 3-m long Kasten corer (Kuehl et al., 1985), and 1.5-m long gravity cores with polycarbonate barrels were collected at 14 of these stations (Fig. 2). Coring locations were targeted based on over 1000 nautical miles of high-resolution (Chirp) subbottom data that was acquired using either an Edgetech 424 or 512i towfish (see Liu et al., 2019). For the 512i towfish deployments, data was acquired using a 0.25-s shot rate, 5-ms pulse length, and a 0.5-to 8.0-kHz swept frequency. A 4–24 kHz frequency range was used during data acquisition when the Edgetech 424 was deployed. Kasten cores were sampled aboard the *Sea Princess* by removing 2-cm thick sections and placing samples in whirl-pack bags for return to the lab and subsequent analyses. Gravity cores were capped and returned intact for processing in the lab.

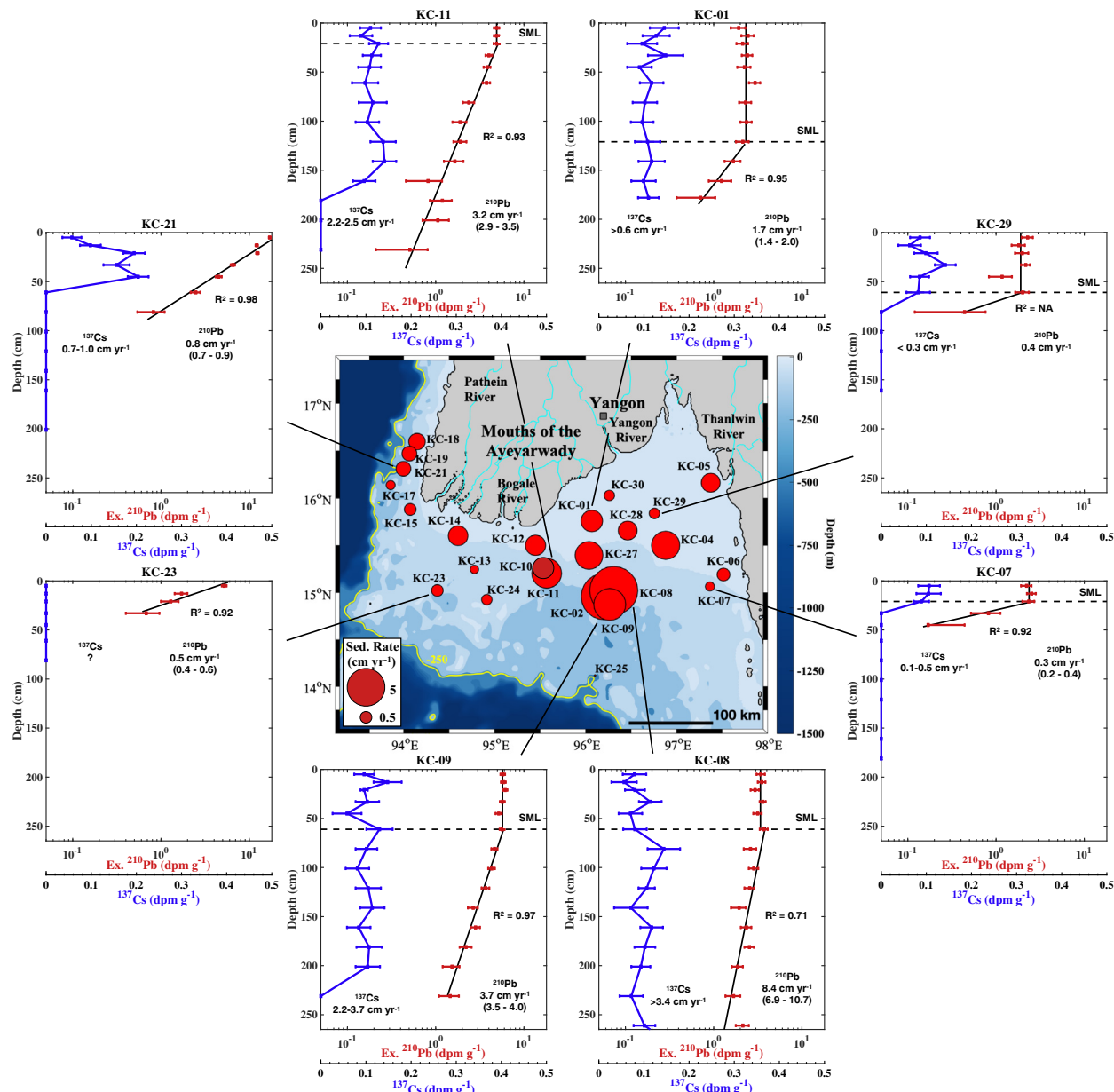


**Fig. 3.** Map (center) with coring locations showing  $^{210}\text{Pb}$ -derived accumulation rates scaled to relative diameter of red circles. Representative excess  $^{210}\text{Pb}$  and  $^{137}\text{Cs}$  activity profiles (perimeter) from geographically distributed sites. (For interpretation of the references to color in this figure legend, the reader is referred to the web version of this article.)

### 3.3. Laboratory analyses

For sediment geochronology, Kasten core samples were dried at 60 °C, and total  $^{210}\text{Pb}$  ( $t_{1/2} = 22.3$  y) and  $^{137}\text{Cs}$  ( $t_{1/2} = 30.17$  y) activities were measured via gamma ray spectroscopy on semi-planar intrinsic germanium detectors coupled with multichannel analyzers, which were calibrated using certified  $^{210}\text{Pb}$  and multi-nuclide standard sources. Dried homogenized sediment samples were sealed in 70-ml petri dishes and were aged for > 21 days to allow  $^{222}\text{Rn}$  decay products  $^{214}\text{Pb}$  (295 and 352 keV) and  $^{214}\text{Bi}$  (609 keV) to achieve secular equilibrium with  $^{226}\text{Ra}$ , and then counted for ~24 h. Self-attenuation corrections were made to total  $^{210}\text{Pb}$  following the approach of Cutshall et al. (1983). Supported lead levels were measured as the average of  $^{226}\text{Ra}$  daughter activities, and excess  $^{210}\text{Pb}$  was then calculated as the total minus supported activity. For applicable sections of downcore profiles, cores linear sediment accumulation rates were calculated using the constant flux-constant sedimentation rate (CF:CS) model (Crozaz

et al., 1964; Krishnaswamy et al., 1971).

Grain size distributions were determined via laser diffraction using a Beckman Coulter LS 13-320. Prior to analysis, wet samples were diluted and sonicated. Grain size fractions were measured as percentage by volume binned into 93 intervals between < 0.375 and 2000  $\mu\text{m}$ . Individual samples were run in triplicate, bins for each run were summed into Sand + Coarse Silt (> 16  $\mu\text{m}$ ), Fine Silt (3.9–16  $\mu\text{m}$ ), and Clay (< 3.9  $\mu\text{m}$ ), and the three runs were averaged for these fractions.

### 3.4. Geophysical data processing

All geophysical data were saved along with corresponding navigation and header data in EdgeTech's native format (JSF). Chirp sonar profiles were processed using the Edgetech Discover Software, seafloor reflections were identified by peak amplitude, and sea-surface heave was removed. Final trace data were plotted with geo-located shot-point tracklines, and incorporated within ArcGIS.

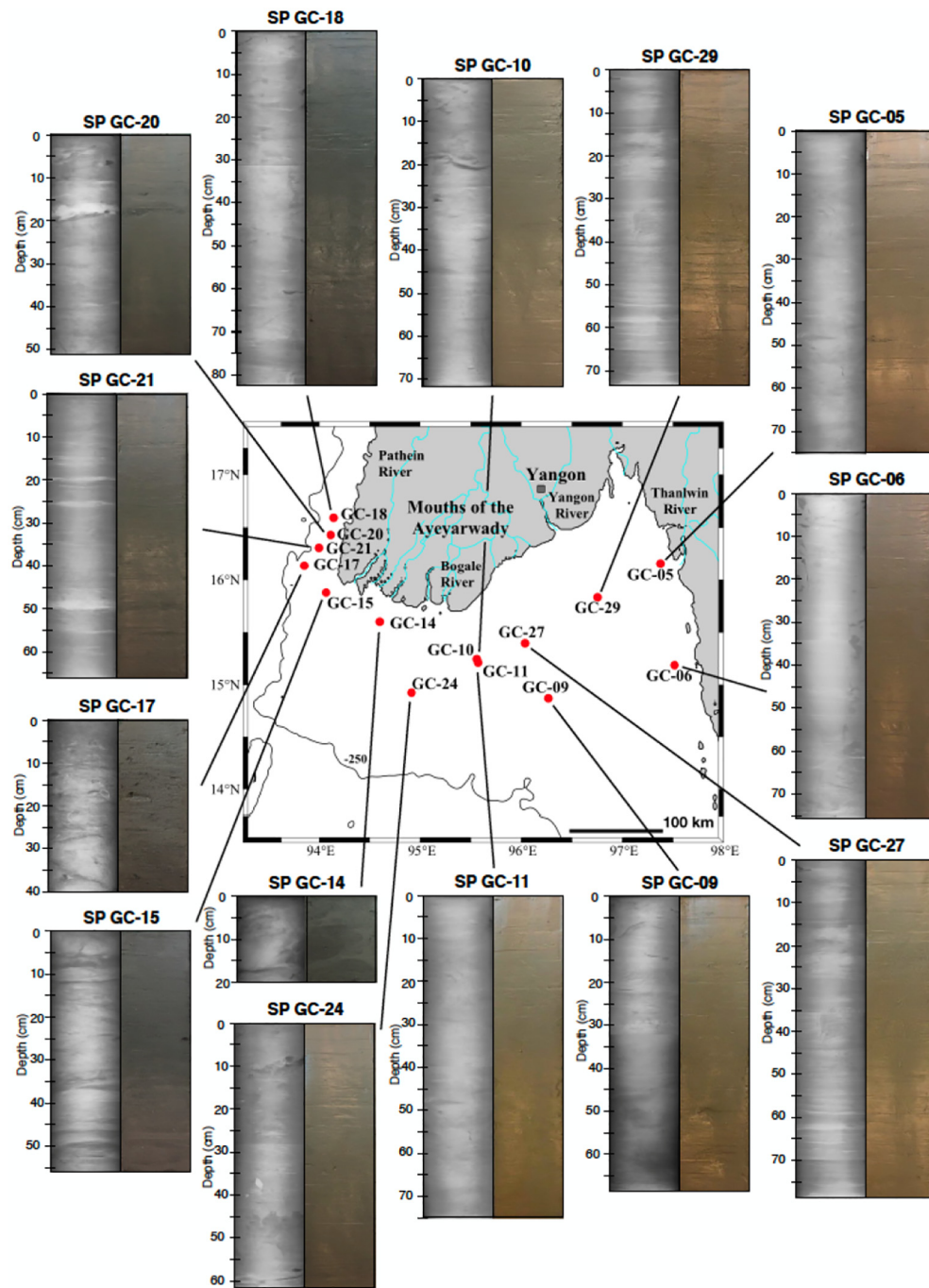


**Fig. 4.** Map (center) showing all station locations where gravity cores were collected. X-radiograph negatives (left) and core photographs (right) for each gravity core (perimeter) showing contrasting internal structure and coloration from east to west. Cores from the eastern portion of the shelf (Gulf of Martaban) generally show homogenous to finely laminated (mm-scale) internal structure in X-radiographs, and distinctive reddish brown coloration in photographs. Cores off the “Mouths of the Ayeyarwady” and along the northwestern shelf appear to contain more sand (cm-scale lighter bands) and shell in X-radiographs, and olive-grey in color. (For interpretation of the references to color in this figure legend, the reader is referred to the web version of this article.)

## 4. Results

### 4.1. Sediment geochronology

Downcore profiles of  $^{137}\text{Cs}$  and  $^{210}\text{Pb}$  show distinctive spatial variations both in character and derived accumulation rate (Fig. 3). Accumulation rates over the broad region of the western shelf are generally  $< 1 \text{ cm y}^{-1}$ , with the exception of a narrow nearshore zone directly off the “Mouths of the Ayeyarwady”, where rates rise slightly to  $1.3 \text{ cm y}^{-1}$ . A distinct depocenter exists in the middle shelf within the Martaban depression, where accumulation rates reach a maximum of  $\sim 10 \text{ cm y}^{-1}$ . Accumulation rates on the shelf seaward of the depocenter decrease rapidly, and are negligible on the outer shelf and near the head of the Martaban canyon. Landward of the depocenter,  $^{210}\text{Pb}$  profiles from the Gulf of Martaban exhibit a pronounced surface mixed

layer (as evidenced by uniform  $^{210}\text{Pb}$  activities) with a thickness ranging from 25 to 120 cm, similar to that reported from the Amazon subaqueous delta (Kuehl et al., 1986). Accumulation rates decrease landward of the depocenter and the two innermost cores (SP-29, 30) exhibit low or negligible net accumulation. Slightly higher rates are observed in the easternmost inner shelf area, directly off the Thanlwin River.

Spatial variations were also observed in specific activities of both  $^{137}\text{Cs}$  and  $^{210}\text{Pb}$  within the study area. Specific surface activities of both radioisotopes are low throughout the Andaman Sea portion of the study area ( $^{210}\text{Pb}$ :  $0.8\text{--}3.5 \text{ dpm g}^{-1}$ ;  $^{137}\text{Cs}$ :  $< 1 \text{ dpm g}^{-1}$ ). Notably,  $^{137}\text{Cs}$  was below detectable limits for four of the sites off the “Mouths of the Ayeyarwady” (SP-12, 13, 23, 24). Conversely, the northwestern sites fronting the Bay of Bengal revealed specific surface activities of  $^{210}\text{Pb}$  up to an order of magnitude greater ( $10.1 \text{ dpm g}^{-1}$  at SP-21) than

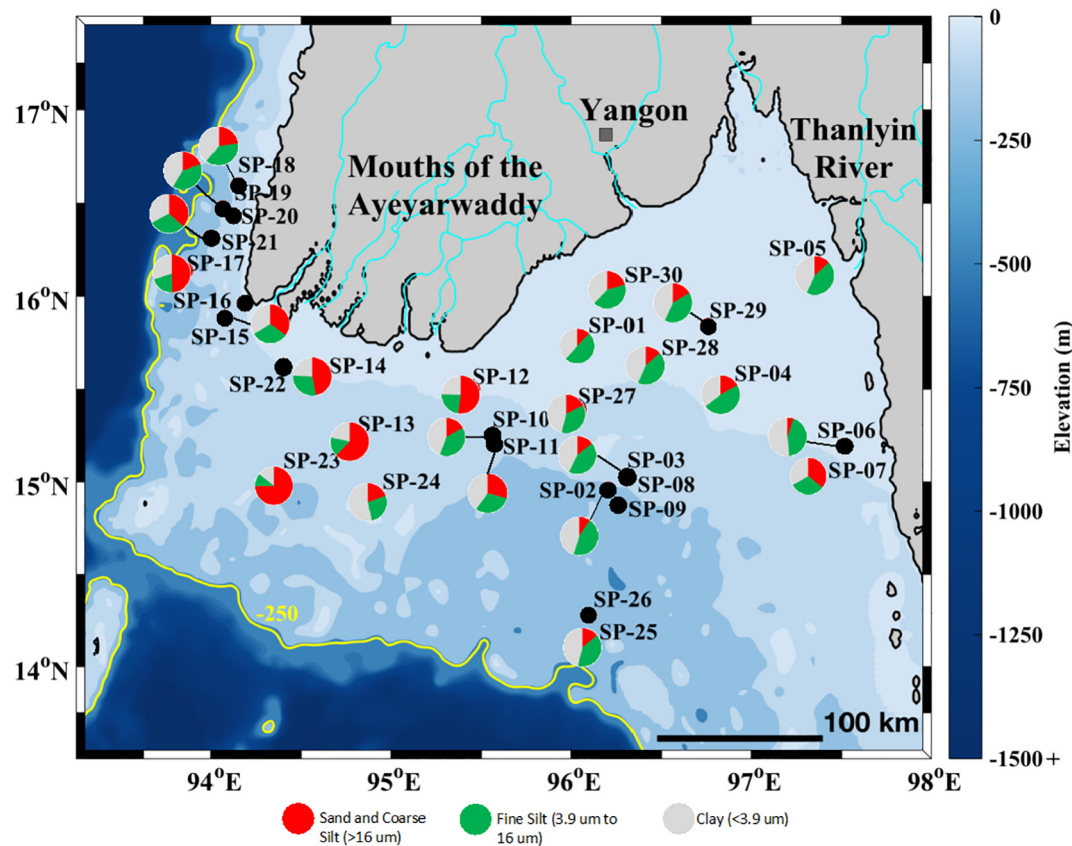


**Fig. 5.** Grain-size pie charts showing fraction of sand + coarse silt, fine silt and clay. Grain-size fractions were derived from down-core averages of 3–5 sample intervals distributed within each kasten core. High clay and fine silt content characterizes the eastern delta (Gulf of Martaban), whereas sand is abundant in the southwestern delta off the “Mouths of the Ayeyarwaddy”. Grain size averages from the northwestern shelf are intermediate between the these two areas.

observed in the Andaman Sea, and relatively high  $^{137}\text{Cs}$  (Fig. 3).

#### 4.2. Sedimentary structure and texture

Gravity cores collected at 14 locations reveal a variety of sedimentary structures, textures and coloration (Fig. 4). Sedimentary structures seen in x-radiographs range from fine silt laminations in mud that resemble tidalites (SP-27, 29), to mottled sandy mud with shell (SP-17). Photographs of freshly split core halves reveal a striking gradient in coloration from east to west. All of the cores taken from the Gulf of Martaban area display a distinctive reddish brown coloration while cores off the “Mouths of the Ayeyarwaddy” and in the northwestern area fronting the Bay of Bengal are olive grey (Fig. 4).

Grain-size distributions for each coring site was determined by averaging results from 3 to 5 depth intervals within each of the cores, typically at least one each from top, middle and bottom of the kasten cores (Fig. 5). Cores from the Gulf of Martaban area generally show a dominance of clay and fine silt, with minor sand + coarse silt. In contrast, the western “Mouths of the Ayeyarwaddy” show abundant sand and coarse silt (with the exception of SP-24). We were unable to recover a gravity core at SP-22, and we presume the sediment there was too coarse for penetration (this was also the case for SP-29 just landward of Martaban Canyon). Coring sites from the northwestern delta fronting the Bay of Bengal are more uniform, and intermediate in size between the Gulf of Martaban and off the “Mouths of the Ayeyarwaddy”, showing subequal amounts of clay, fine silt, and sand + coarse silt.

#### 4.3. High-resolution seismic

Representative Chirp profiles show three distinct regions of contrasting stratigraphic architecture (Figs. 6, 7, 8). A thick (up to 50 m)

Holocene mud wedge extends from the Gulf of Martaban across the mid-shelf region (Fig. 6). The mud-wedge pinches out at about 130 m water depth, and the outer shelf is characterized by block faulting of suspected older (late Pleistocene) strata. Off the “Mouths of the Ayeyarwaddy” the subbottom penetration is generally only a few meters and the seafloor appears more chaotic, with a few areas of thin acoustically transparent material (muds) (Fig. 7). Along the northwestern region, a uniform stratified mud drape up to 20-m thick nearshore extends across the entire shelf and thins seaward on the slope to limit of the survey (~300 m water depth) (Fig. 8). A more detailed discussion of geophysical results is presented in Liu et al. (2019).

#### 4.4. CTD profiles

CTD casts from stations outside of the Gulf of Martaban looked as expected, in that conductivity, which is usually interpreted to indicate salinity, increased with depth. For example the CTD cast from Station 27 showed increasing conductivity with depth (Fig. 9C). Note that the OBS from this station also recorded low backscatter indicating low suspended sediment concentrations (Fig. 9C). In contrast, the CTD data from nearby Station 1 had a conductivity profile that decreased in the bottom boundary layer, and the OBS for this station recorded high backscatter near the seabed (Fig. 9B). All of the CTD casts were analyzed to characterize the conductivity and turbidity over the study area (Fig. 9A). Stations that had high OBS near-bed readings (backscatter  $> 1$  V; plotted using circles in Fig. 9A) coincided with stations for which conductivity decreased in the bottom boundary layer (black triangles in Fig. 9A). These included four of the five stations sampled in the Yangon River, and the three shallowest locations from the Gulf of Martaban (Fig. 9A). The conductivity readings at these stations may have been reduced by high concentrations of suspended sediment, and

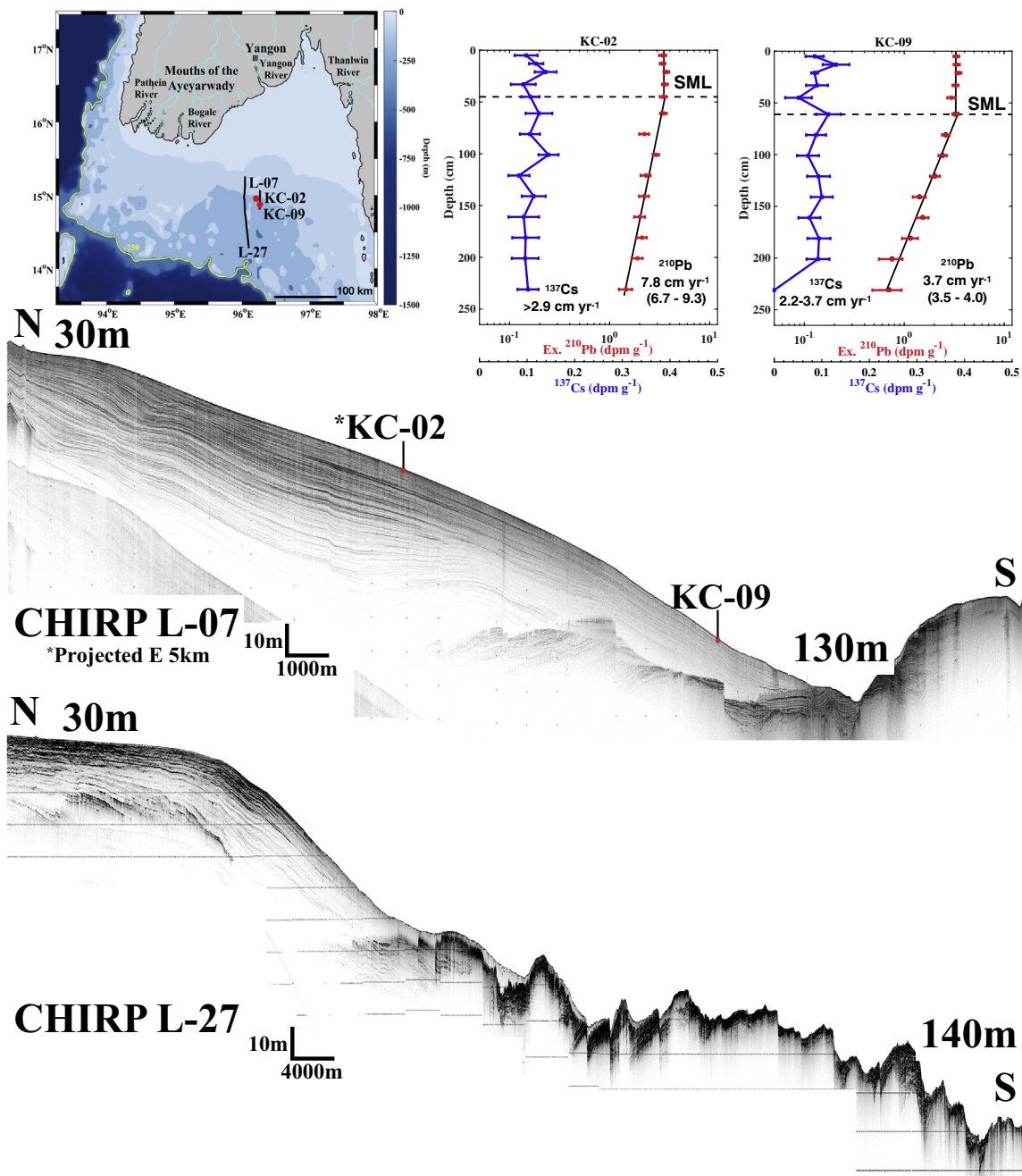


**Fig. 6.** Map (upper left) showing location of Chirp lines 7 and 27 (bottom panels), and near-line coring locations (red dots). Chirp profiles across the eastern mid-shelf show a thick (up to 50 m) mud wedge that pinches out on the middle shelf. The mid- to outer-shelf is highly reflective and reveals a blocky surface morphology ( $> 10$  m relief) consistent with the presence of relict sands exposed in a pull-apart basin associated with the Sagaing fault. Sediment accumulation rates from  $^{210}\text{Pb}$  and  $^{137}\text{Cs}$  profiles (upper right panels) show a decrease from the middle of the steeply dipping mud wedge (foreset; KC-02) toward the pinch out (KC-09). (For interpretation of the references to color in this figure legend, the reader is referred to the web version of this article.)

the reduced conductivity is interpreted to represent the presence of high suspended-sediment concentrations (fluid mud?), which has been reported to affect the conductivity sensor (Held et al., 2014). Stations for which the OBS readings were not elevated showed either conductivity that increased with depth, or little variation in conductivity with depth (white triangles and grey squares, respectively in Fig. 9A). CTD casts from the Gulf of Martaban generally show a stratified water column in water depths  $> 30$  m with shallower depths showing a well-mixed water column.

#### 4.5. Wave climate

The Wave Watch III global wave model estimates of wave heights were averaged for January and August 2016 (Fig. 10). Though it has relatively low spatial resolution, the global Wave Watch III® model provides insight into the spatial and seasonal wave climate within the study area. Wave heights are generally higher, as expected, during the SW monsoon in August, when the northwestern and "Mouths of the Ayeyarwady" areas are subjected to significant wave heights approaching 2 m (Fig. 10a). Wave energy is reduced during January, but is still significant in the western areas (Fig. 10b). Wave model estimates

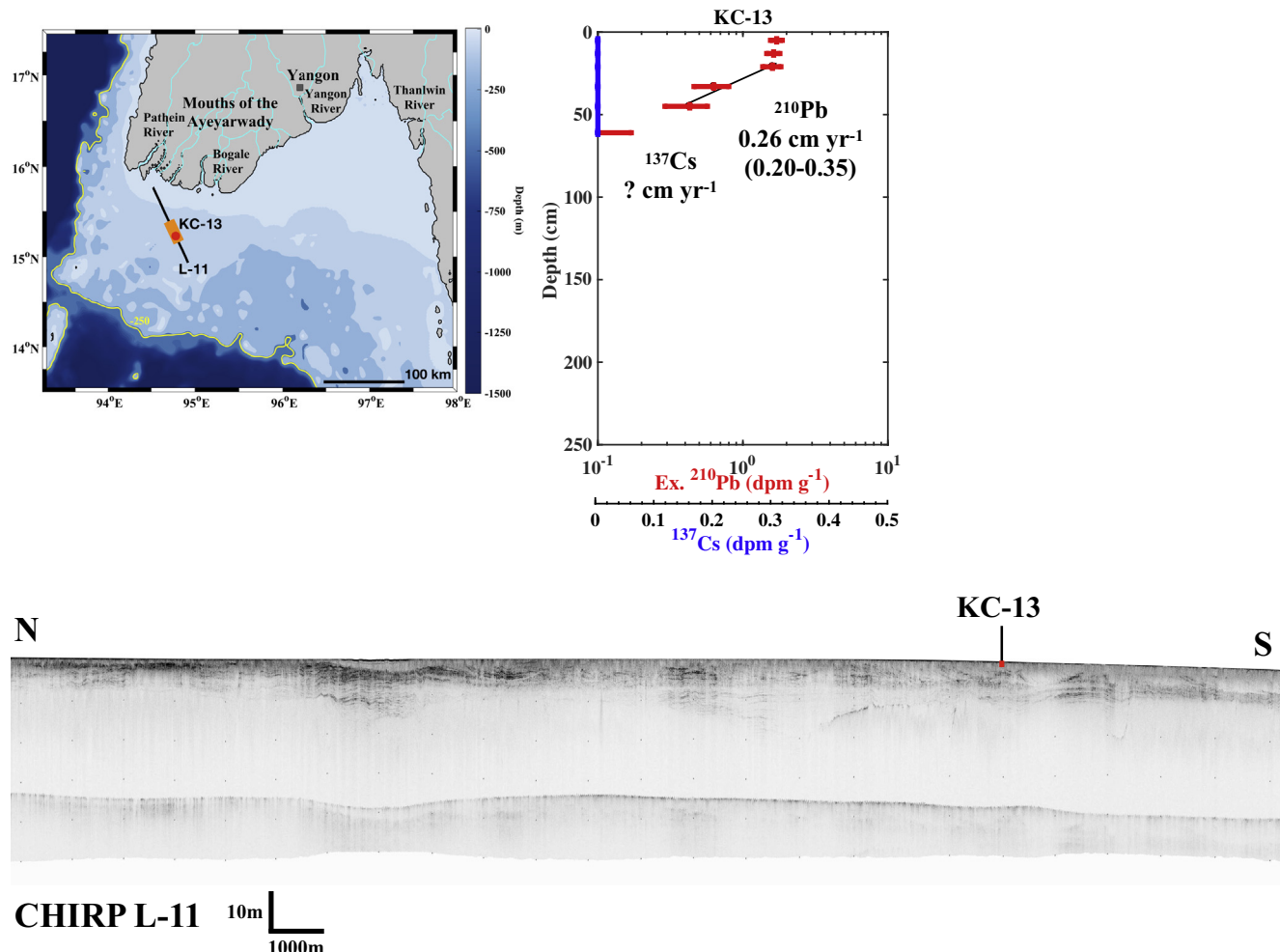


**Fig. 7.** Map (upper left) showing location of Chirp line 11 (bottom panel) and near-line coring location (red dot). This characteristic Chirp profile across the inner shelf off the western “Mouths of the Ayeyarwady” shows shallow acoustic penetration and irregular near-surface stratigraphy suggestive of a sandy substrate with localized muddy patches. Seabed profiles of  $^{210}\text{Pb}$  and  $^{137}\text{Cs}$  show shallow penetration of  $^{210}\text{Pb}$  and low accumulation rate ( $0.26 \text{ cm yr}^{-1}$ ), and the absence of detectable  $^{137}\text{Cs}$ , possibly a result of the coarser sediment texture (see Fig. 5) in this region. (For interpretation of the references to color in this figure legend, the reader is referred to the web version of this article.)

for both seasons show low wave heights in the Gulf of Martaban, suggesting low wave energy throughout the year in this region.

## 5. Discussion

The offshore Ayeyarwady delta in the northern Andaman Sea presents as a compound geomorphic feature with dramatically contrasting morphologies and sediment dispersal patterns to the west and east of the Sagaing fault (Fig. 11). Farther west, along the northwestern part of the study area fronting the Bay of Bengal, the shelf is much narrower and more uniform in character. These three distinct regions are explored in the following sections.

### 5.1. Gulf of Martaban and Martaban depression

In the central and eastern delta, the Martaban depression accommodates the growth of a thick Holocene mud wedge (subaqueous delta) that has prograded seaward to the mid-shelf. Sediment texture for the subaqueous delta is dominated by fine silt and clay. The Chirp sonar data indicates the thickness of the mud accumulation in the depocenter is  $> 50 \text{ m}$  (Fig. 6, and Liu et al., 2019). Sediment accumulation rates reach  $10 \text{ cm yr}^{-1}$  in the foreset region of the subaqueous delta, indicating rapid seaward progradation. Farther south, the wide

continental shelf is characterized by the exposure of late Pleistocene fault blocks and relict sandy sediment. Chirp sonar profiles from the Martaban Canyon at 300–500 m water depths indicate there are no modern sediments in the canyon (see Line-24 in Liu et al., 2019), which likely indicates there is little or no escape of modern river sediment to the Andaman Trough during the present sealevel highstand. This conclusion contrasts with that of Rao et al. (2005), who suggested that the canyon may be an active conduit for off-shelf transport, based primarily on water column measurements that showed a low SSC ( $< 0.5 \text{ mg/l}$ ) near bottom layer extending offshore over the canyon. While we acknowledge the possibility of some offshore sediment escape in such a nepheloid layer, the absence of any connectivity along the seafloor between the modern shelf mud deposit and the canyon suggests the Martaban Depression traps the vast majority of the modern river derived sediment in the northern Andaman Sea area.

Based on earlier satellite observations, the eastern inner shelf (Gulf of Martaban) has previously been described as the world's largest area of persistently high surface turbidity (Ramaswamy et al., 2004). Our water column and seabed observations and measurements suggest the presence of expansive fluid muds and deep seabed mixing in this area, with significant implications for geochemical cycling of the huge quantities of organic carbon supplied by the rivers and offshore primary production. We suggest that the distinctive reddish brown color of cores

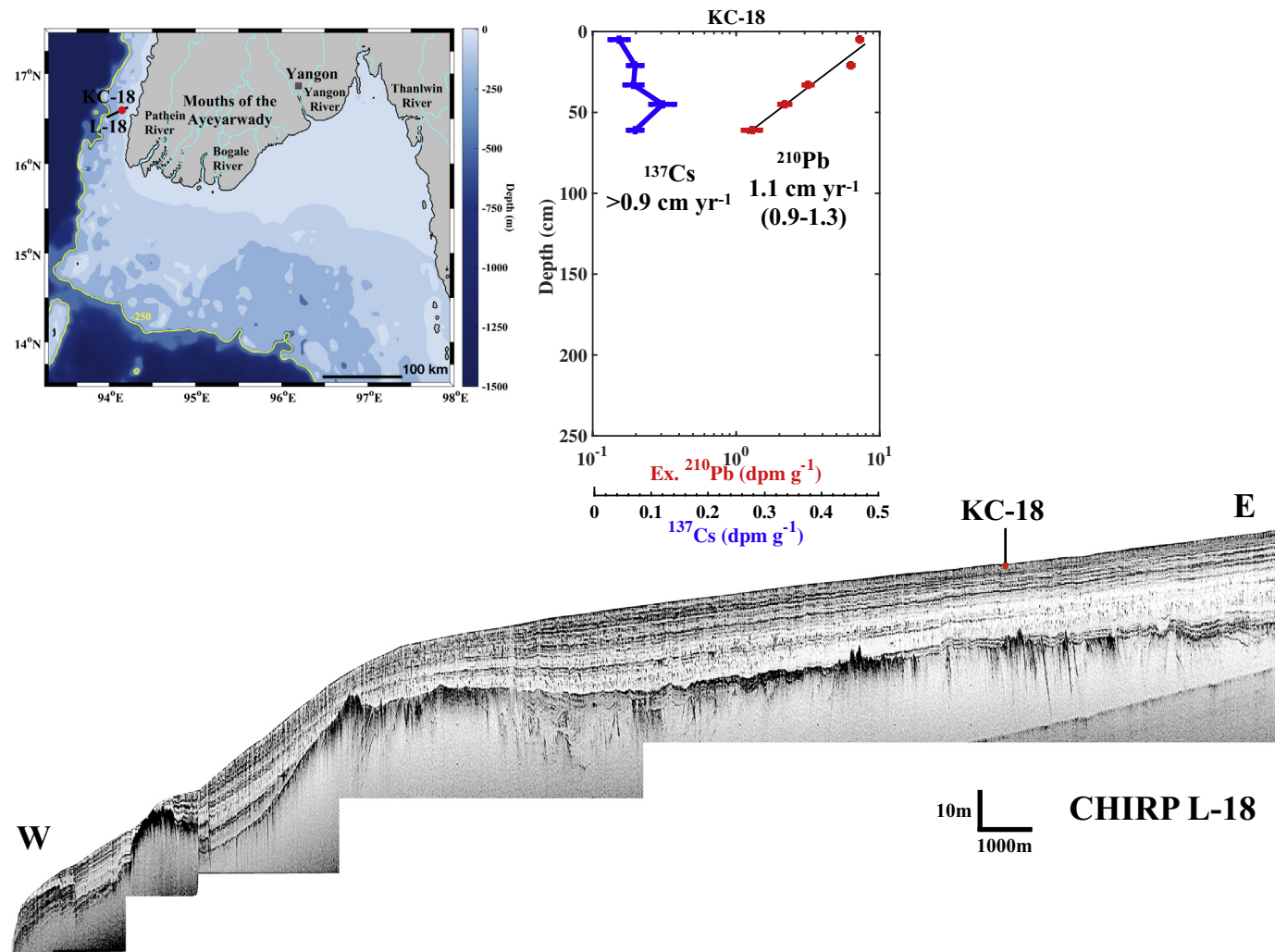


**Fig. 8.** Map (upper left) showing location of Chirp line 18 (bottom panel), and near-line coring location (red dot). This typical Chirp profile across the narrow northwestern shelf reveals a stratified mud drape (~20 m thick) across the shelf that extends onto the slope and thins seaward. Sediment accumulation rate from  $^{210}\text{Pb}$  and  $^{137}\text{Cs}$  profiles on KC-18 is  $\sim 1 \text{ cm yr}^{-1}$ , typical for this region and order of magnitude lower than the central eastern shelf (see Fig. 3). (For interpretation of the references to color in this figure legend, the reader is referred to the web version of this article.)

from the Gulf of Martaban may be a result of frequent re-oxidation and formation of diagenetic S-poor minerals, similar to that observed for the Amazon shelf region by [Aller and Blair \(1996\)](#).

Based on the global WaveWatch III® model results, wave action is reduced in the Gulf of Martaban. Furthermore, the WaveWatch III® model does not fully account for shallow water wave processes; or take into consideration the presence of fluid muds, which would additionally reduce wave energy through wave damping in this thixotropic medium (e.g., [Winterwerp et al., 2007](#)). Therefore, during typical conditions, the dominant energy source for sediment resuspension and fluid mud formation is likely from tidal currents. This idea is supported by satellite observations of surface suspended sediment, that show waxing and waning of the high turbidity area in concert with tidal modulation (i.e., roughly a doubling of the area from 20,000 km $^2$  to 40,000 km $^2$  from neap to spring tide) ([Ramaswamy et al., 2004](#)). While tidal resuspension dominates the suspended sediment signal during normal conditions, we cannot rule out the possible importance of storm swell generated by major cyclones.

The seasonal persistence of high turbidity surface waters in the Gulf ([Ramaswamy et al., 2004](#)) furthermore suggests that local circulation acts to at least partially trap fine-grained sediments in this region. One possible mechanism could be that fresher water at the surface leads to estuarine-like flow on the shelf, where more saline bottom currents

move landward underneath a seaward spreading surface flow. Our CTD casts from December (low river flow) show a stratified water column in the mid-shelf region (> 30 m water depth), with more saline bottom waters overlain by fresher water there ([Fig. 9A](#)). Tidal mixing in shallower waters (< 20 m water depth) during this period of low river discharge create a well-mixed water column nearshore ([Fig. 9A](#)), indicating the salt wedge intersects the bed somewhere between the 30- and 20-m isobaths during low flow, landward of the topset/foreset transition. Fortnightly changes in tidal amplitude, as well as seasonal changes in freshwater input and winds would cause such a front to migrate across the shallow Gulf, potentially resulting in a migrating zone of deposition/erosion, consistent with our seabed observations of a pronounced surface mixed layer. High accumulation rates in Martaban depression suggest periodic release of trapped nearshore sediment to deeper waters. This could be accomplished either by wind events that force the rapid migration of fresh surface waters and breakdown of the frontal system; or during periods of high river discharge, when the front may extend seaward beyond the topset/foreset transition of the subaqueous delta, effectively releasing a cascade of dense near-bottom suspensions into the deeper areas of the middle shelf.

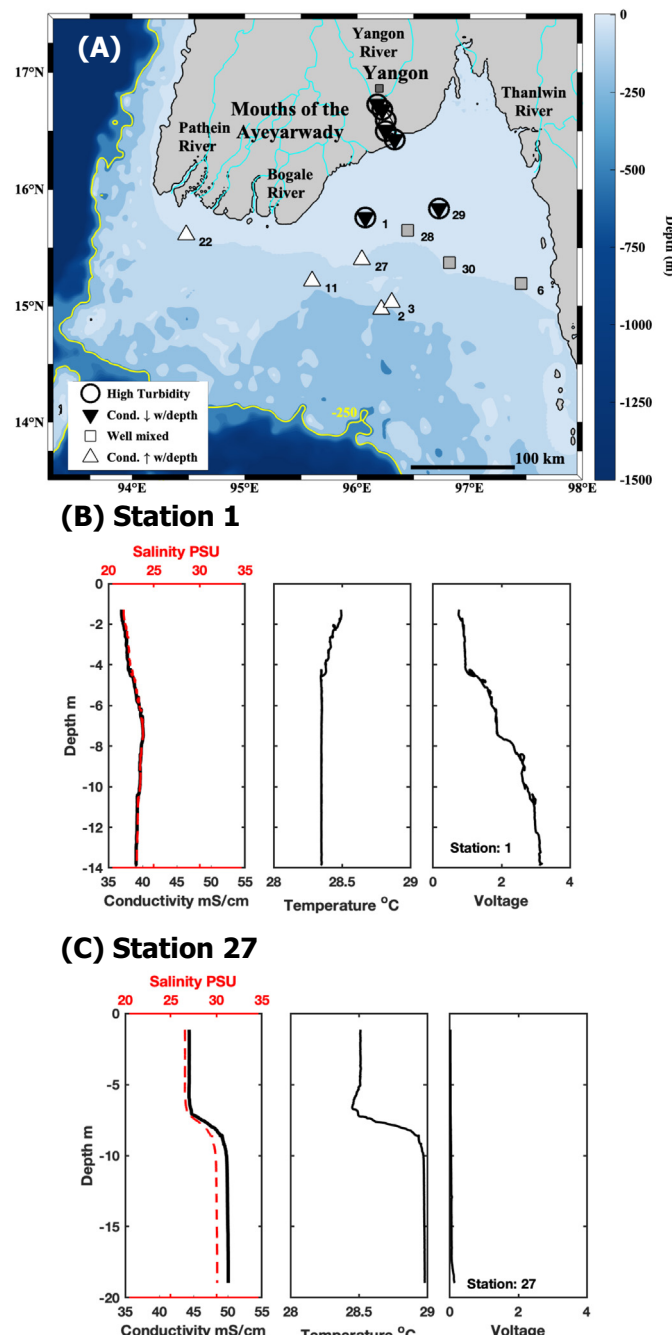


**Fig. 9.** (A) Map showing locations of CTD profiles including Stations 1 and 27. Station locations where the OBS indicated high turbidity are circled. Stations where conductivity decreased with depth shown as black triangles. Stations where conductivity increased with depth shown as white triangles. Locations where conductivity showed little change with depth are shown as grey squares. (B) and (C): CTD data from stations number 1 and 27, respectively. The CTD data shown relative to depth below the water surface (vertical axis). Left-most panels show measured conductivity (black line, bottom axis) and salinity inferred from conductivity (red line, top axis). Middle panels show temperature. Right panels show OBS Voltage, where higher numbers indicate more backscatter and turbidity. (For interpretation of the references to color in this figure legend, the reader is referred to the web version of this article.)

## 5.2. “Mouths of the Ayeyarwady”

The shelf ramp seaward of the Ayeyarwady river mouths along the southwestern part of the delta presents a marked contrast to the eastern Gulf of Martaban and Martaban depression. Despite major sediment

input from the Ayeyarwady, accumulation rates in this area are up to an order of magnitude lower than those observed in the Gulf of Martaban. Sediment is dominated by sand and coarse silt, with minor clay content (Fig. 5), which likely explains the low seabed radioisotope activities and, in some cases, the absence of detectable  $^{137}\text{Cs}$  (e.g., KC-23; Fig. 3). Chirp profiles show only limited subsurface penetration with some thin minor patches of acoustically transparent sediment (Fig. 7, and Liu et al., 2019), further supporting the notion of a reduced modern mud accumulation in this region. These observations, coupled with the lack of recent shoreline progradation (Hedley et al., 2010), suggest that fine sediments delivered to and deposited on the southwestern shelf are removed and transported elsewhere. Surface gravity waves provide a major energy source for sediment resuspension off the “Mouths of the Ayeyarwady” (Fig. 10) which limits the retention of fine-grained sediments (the bulk of the riverine sediment load) on the shelf in this area. This area is open to swell from the Bay of Bengal, and acts as a large-scale promontory that serves to focus wave energy. Consistent with the findings of Rao et al. (2005), we suspect that the bulk of fine sediments in suspension on the southwestern shelf are carried eastward into the Gulf of Martaban by surface currents during the Southwest monsoon, the period of highest river discharge and highest wave action. During the Northwest monsoon, this situation may reverse, with suspended fines moving westward and perhaps contributing to the development of the mud drape observed in the northwestern region of the delta.

Over the late Holocene, the delta plain (and shoreline) of the southwestern delta have prograded > 200 km seaward, belying the observations of more recent shoreline stability (Hedley et al., 2010). One possible explanation for the reduced recent shoreline progradation could be related to the presence of the Indo-Burman mountain range that borders the northwestern coast. During the early to mid-Holocene, the Indo-Burman range would have created a major embayment along its eastern side, presumably sheltering the area from major swell originating in the Bay of Bengal and allowing the retention of fine sediment, promoting rapid progradation. As the shoreline moved farther seaward, exposure to wave action would increase, leading to a reduction in the progradation rate. At present, the shoreline has advanced to the southern edge of the subaerially exposed Indo-Burman range, which no longer offers protection along its southern front. As a result of this varying sheltering afforded by the Indo-Burman range over the mid- to late-Holocene, we posit that the southwestern delta may have evolved to a geomorphic equilibrium, where at present fine sediment inputs are balanced by removal by oceanographic processes.

## 5.3. Northwestern shelf area

The relatively narrow margin along the western side of the Indo-Burman range displays a ~20-m thick Holocene mud deposit that extends across the shelf, thinning farther seaward to at least the upper slope (~300 m water depth), the extent of our survey (Fig. 8, and Lines 15–19 in Liu et al., 2019). Shelf accumulation rates are moderate ( $\sim 1 \text{ cm y}^{-1}$ ), and sand + coarse silt contents are intermediate between those of recent sediments from the Gulf of Martaban and “Mouths of the Ayeyarwady”. Fine-scale sedimentary structure observed in x-radiographs show denser (sand + silt) layers that contain sharp basal contacts suggestive of event (storm?) layers (Fig. 4). Given that this region faces the open Bay of Bengal, these storm layers could reflect large swell events from major cyclones that move northward over the Bay toward India and Bangladesh.

In contrast with Gulf of Martaban, no cross-shelf prograding subaqueous delta is observed for this mud deposit; rather, the deposit exhibits a stratified “mud drape”, suggesting a more energetic (dispersive) and along-shelf transport regime. Some suspended sediment may escape westward from the northern Andaman Sea during the northeast monsoon, and could move northward along the coast supplying sediment to this area (Rao et al., 2005). Alternatively, sediments accumulating on the northwestern shelf could potentially be derived from a

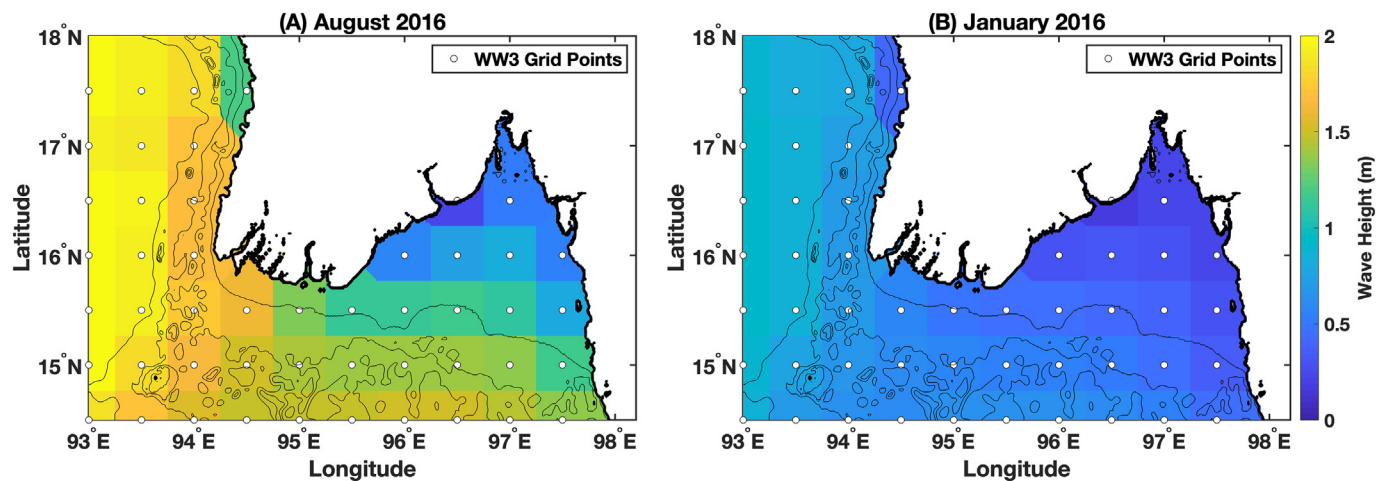


**Fig. 10.** Maps of Wave Watch III® model wave heights calculated for the study area for (A) August 2016 (SW monsoon) high-energy periods and (B) January 2016 (NE monsoon) low energy period. White dots show locations of WW3 model calculations, which were interpolated spatially using nearest-neighbor. Bathymetric contours (black lines) drawn at 25, 50, 100, and 1000 m. During both periods, wave heights are highest along the northwestern and western regions, and are reduced in the eastern Gulf of Martaban. High wave energy (and tides) in the western regions may explain coarser texture shelf sediment in these regions (see Fig. 5), with winnowing and transport of fines toward the east, during the SW monsoon.

## Conceptual Model of Offshore Ayeyarwady Delta

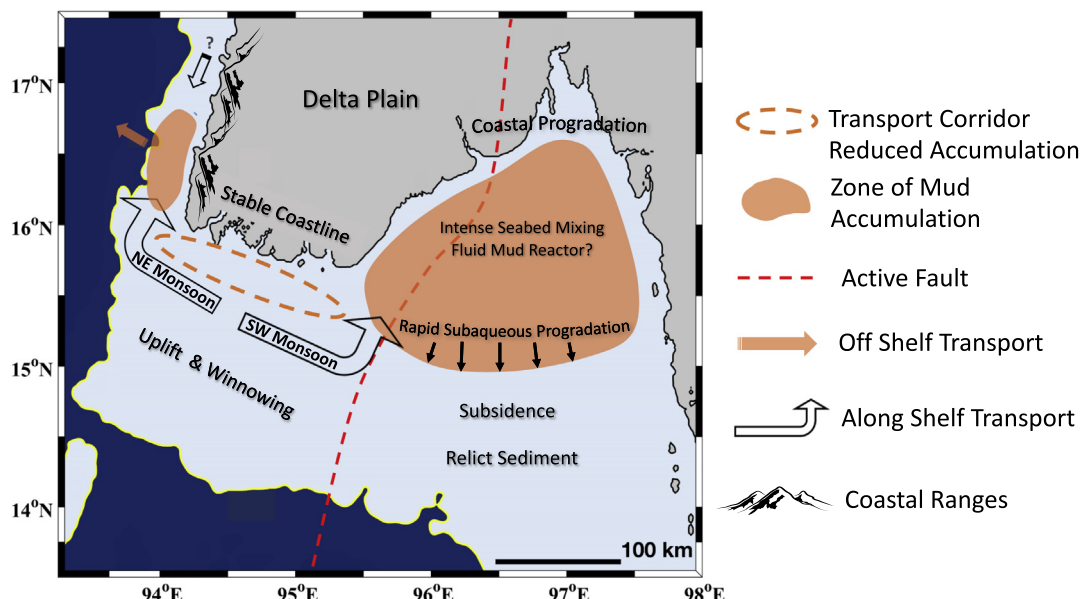


**Fig. 11.** Cartoon showing conceptual model of sediment dispersal and accumulation off the Ayeyarwady delta (see discussion for more complete explanation). The largest zone of mud deposition and accumulation is found in the eastern Gulf of Martaban and Martaban depression, which is sheltered from wave resuspension. Sediment trapping and strong tidal currents in the shallow Gulf result in a mixed surface seabed layer, and extremely high suspended-sediment concentrations. Farther seaward, tectonic accommodation in the Martaban depression leads to high accumulation and a rapidly prograding mud wedge. The western region is strongly affected by waves, leading to temporary deposition off the “Mouths of the Ayeyarwady” and subsequent winnowing and transport of much of the fine river-derived sediment toward the east during the SW monsoon, and possibly westward during the NE monsoon. The mud patch on the northwestern shelf fronting the Bay of Bengal may be composed of a combination of Ayeyarwady sediment delivered during the NE monsoon, and local sources from the mountainous Indo-Burman range.

northern source or from small rivers entering the area from the adjacent Indo-Burman range. A hydrodynamic model for the northern Bay of Bengal shows the presence of a coastal current flowing southward along Bangladesh and Myanmar during late winter (Dandapat et al., 2018). Given that the Ganges-Brahmaputra is a major source of sediment in the northern Bay of Bengal, it seems plausible that the mud drape along the northwestern portion of our study area could be sourced from these giant rivers. However, analyses of Sr and Nd isotopes from surface

sediments in this area shows no evidence of a significant Ganges-Brahmaputra source; rather, the provenance of these sediments is more likely attributed to a mixture of Ayeyarwady and local sources from the Rakhine coast (Damodararao et al., 2016). A mixed sediment source in this region could explain observed differences in sediment coloration. Whereas the modern muds accumulating in the Andaman Sea display a distinctive reddish brown color, sediments from the northwestern coast are a more uniform olive grey (Fig. 4). Regardless of the source of

sediment, the fact that the mud drape extends beyond the shelf break indicates that some sediment escapes from the shelf to the deeper Bay of Bengal. Sediment escaping from the shelf could play an important role in carbon sequestration in the Indian Ocean, as this lithogenic matter serves as ballast to enhance settling of organic matter to the sea floor (Rixen et al., 2019). However, the quantity of material escaping and the extent of its dispersal are unknown.

## 6. Conclusions

- 1) Sediment dispersal and accumulation on the shelf off of the Ayeyarwady Delta in the northern Andaman Sea and Bay of Bengal are controlled by a combination of riverine, atmospheric, oceanographic and geologic factors, including: seasonal variations in sediment input; reversing monsoon winds and circulation patterns; strong forcing by tides and waves, and tectonic uplift/subsidence west/east of the N-S trending Sagaing fault.
- 2) Maximum sediment accumulation rates of  $\sim 10 \text{ cm y}^{-1}$  are observed in the foreset region of the subaqueous delta (clinoform) that is prograding into the tectonically controlled Martaban Depression (up to 130 m water depth) east of the Sagaing fault. Seaward of the prograding mud clinoform within the Martaban depression, accumulation rates are nil (relic sediments) and there appears to be no connectivity with the Martaban Canyon at present, which was likely a major conduit for off shelf transport during low sea-level conditions. Accumulation rates in other areas of the shelf surrounding the delta are typically  $\sim 1 \text{ cm y}^{-1}$ .
- 3) The extensive shallow (topset) region of the Gulf of Martaban is characterized by deep ( $\sim 1 \text{ m}$ ) physical mixing of the seabed and reduced net accumulation rates. Frequent and deep re-oxidation of pore waters by tidally-driven sediment resuspension likely provides the conditions for Fe mineral formation and a distinctive reddish-brown coloration of the sediments. These conditions are also likely unfavorable for efficient burial of organic matter.
- 4) The shelf (ramp) off of the western "Mouths of the Ayeyarwady" is characterized by a relatively narrow nearshore ( $< 40 \text{ m}$  water depth) mud belt with higher sand and silt content offshore, and accumulation rates typically  $< 1 \text{ cm y}^{-1}$ . This area of the delta is subject to frequent wave resuspension (especially during the SW monsoon), when most of the fine-grained sediments delivered to the river mouths are winnowed and transported eastward to the Gulf of Martaban.
- 5) The western most area adjacent to the Bay of Bengal is characterized by a mud drape extending across the entire shelf to slope with accumulation rates of  $\sim 1 \text{ cm y}^{-1}$ . This area likely receives some sediment from small streams draining the western Indo-Burman range, along with a mixture of Ayeyarwady sediment that may be transported westward during the NE monsoon.

## Acknowledgements

This research was supported by the National Science Foundation, USA grants OCE-1737221 (PIs Kuehl and Harris), and OCE-1737287 (PI Liu). The authors express their deepest appreciation to the students and faculty at University of Yangon and Mawlamyine University for their support and participation in the research cruise. We also thank the Captain and crew of the *Sea Princess*, as this study would not have been possible without their hard work and dedication in support of our sampling efforts.

## References

Aller, R.A., Blair, N.E., 1996. Sulfur diagenesis and burial on the Amazon shelf: major control by physical sedimentation processes. *Geo-Mar. Lett.* 16, 3–10.

Awasthi, N., Ray, J.S., Singh, A.K., Band, S.T., Rai, V.K., 2014. Provenance of the Late Quaternary sediments in the Andaman Sea: implications for monsoon variability and ocean circulation. *Geochem. Geophys. Geosyst.* 15, 3890–3906.

Basset, M., Anthony, E.J., Dussouillez, P., Goichot, M., 2017. The impact of Cyclone Nargis on the Ayeyarwady (Irrawaddy) River delta shoreline and nearshore zone (Myanmar): towards degraded delta resilience? *Compt. Rendus Geosci.* 349, 238–247. <https://doi.org/10.1016/j.crte.2017.09.002>.

Bianchi, T.S., Allison, M.A., 2009. Large-river delta-front estuaries as natural "recorders" of global environmental change. *Proc. Natl. Acad. Sci.* 106, 8085–8092.

Bianchi, T.S., Allison, M.A., Cai, W.J., 2013. An introduction to the biogeochemistry of river-coastal systems. In: Bianchi, T.S., Allison, M.A., Cai, W.J. (Eds.), *Biogeochemical Dynamics at Major River-Coastal Interfaces Linkages with Global Change*. Cambridge University Press, pp. 3–18.

Bird, M.I., Robinson, R.A.J., Win Oo, N., Maung Aye, M., Lu, X.X., Higgitt, D.L., Swe, A., Tun, T., Lhaing Win, S., Sandar Aye, K., Mi Mi Win, K., Hoey, T.B., 2008. A preliminary estimate of organic carbon transport by the Ayeyarwady (Irrawaddy) and Thanlwin (Salween) Rivers of Myanmar. *Quat. Int.* 186, 113–122.

Chapman, H., Bickle, M., Thaw, S.H., Thiam, H.N., 2015. Chemical fluxes from time series sampling of the Irrawaddy and Salween Rivers, Myanmar. *Chem. Geol.* 401, 15–27.

Clift, P.D., Giosan, L., Henstock, T.J., Tabrez, A.R., 2014. Sediment storage and reworking on the shelf and in the Canyon of the Indus River-Fan System since the last glacial maximum. *Basin Res.* 26, 183–202.

Crozaz, G., Picciotto, E., De Breuck, W., 1964. Antarctic snow chronology with  $\text{Pb}^{210}$ . *J. Geophys. Res.* 69, 2597–2604. <https://doi.org/10.1029/JZ069i012p02597>.

Curry, J.R., 2005. Tectonics and history of the Andaman Sea region. *J. Asian Earth Sci.* 25, 187–232.

Curry, J.R., Moore, D.G., Lawver, L.A., Emmel, F.J., Raitt, R.W., 1979. Tectonics of the Andaman Sea and Burma. In: Watkins, J., Montadert, L., Dickenson, P.W. (Eds.), *Geological and Geophysical Investigations of Continental Margins*. American Association of Petroleum Geologists Memoir 29, pp. 189–198.

Cutshall, N.H., Larsen, I.L., Olsen, C.R., 1983. Direct analysis of  $^{210}\text{Pb}$  in sediment samples: self-absorption corrections. *Nucl. Instrum. Methods Phys. Res.* 206, 309–312.

Damodararao, K., Singh, S.K., Rai, V.K., Ramaswamy, V., Rao, P.S., 2016. Lithology, monsoon and sea-surface control on provenance, dispersal and deposition of sediments over the Andaman continental shelf. *Front. Mar. Sci.* 3, 1–15.

Dandapat, S., Chakraborty, A., Kuttippurath, J., 2018. Interannual variability and characteristics of the East India Coastal current associated with Indian Ocean Dipole events using a high resolution regional ocean model. *Ocean Dyn.* 68, 1321–1334.

Fritz, H.M., Blount, C.D., Thwin, S., Thu, M.K., Chan, N., 2009. Cyclone Nargis storm surge in Myanmar. *Nat. Geosci.* 2, 448–449.

Furuichi, T., Win, Z., Wasson, R.J., 2009. Discharge and suspended sediment transport in the Ayeyarwady River, Myanmar: centennial and decadal changes. *Hydrol. Process.* 23, 1631–1641.

Garzanti, E., Wang, J.-G., Vezzoli, G., Limonta, M., 2016. Tracing provenance and sediment fluxes in the Irrawaddy River basin (Myanmar). *Chem. Geol.* 440, 73–90.

Giosan, L., Naing, T., Tun, M.M., Clift, P.D., Filip, F., Constantinescu, S., Khonde, N., Blusztajn, J., Buylaert, J.-P., Stevens, T., Thwin, S., 2018. On the Holocene evolution of the Ayeyarwady megadelta. *Earth Surf. Dyn.* 6, 451–466.

Grill, G., Lehner, B., Thieme, M., Geenen, B., Tickner, D., Antonelli, F., Babu, S., Borrelli, P., Cheng, L., Crochetiere, H., Ehalz Maceo, H., Filgueiras, R., Goichot, M., Higgins, J., Hogan, Z., Lip, B., McClain, M.E., Meng, J., Mulligan, M., Nilsson, C., Olden, J.D., Opperman, J.J., Petry, P., Reidy Liermann, C., Sáenz, L., Salinas-Rodríguez, S., Schelle, P., Schmitt, R.J.P., Snider, J., Tan, F., Tockner, K., Valdujo, P.H., van Soesbergen, A., Zarfl, C., 2019. Mapping the world's free-flowing rivers. *Nature* 569. <https://doi.org/10.1038/s41586-019-1111-9>.

Gupta, H., Kao, Shuh-Ji, Dai, M., 2012. The role of mega dams in reducing sediment fluxes: a case study of large Asian rivers. *J. Hydrol.* 464–465, 447–458.

Hedley, P.J., Bird, M.I., Robinson, R.A.J., 2010. Evolution of the Irrawaddy delta region since 1850. *Geogr. J.* 176, 138–149.

Held, P., Kegler, P., Schrottke, K., 2014. Influence of suspended particulate matter on salinity measurements. *Cont. Shelf Res.* 85, 1–8.

Khan, P.K., Chakraborty, P.P., 2005. Two-phase opening of Andaman Sea: a new seismotectonic insight. *Earth Planet. Sci. Lett.* 229, 259–271.

Korus, J.T., Fielding, C.R., 2015. Enhanced bioturbation on the down-drift flank of a Turonian asymmetrical delta: implications for seaway circulation, river nutrients and facies models. *Sedimentology* 62.

Krishnaswamy, S., Lal, D., Martin, J.M., Meybeck, M.M., 1971. Geochronology of lake sediments. *Earth Planet. Sci. Lett.* 11, 407–414.

Kuehl, S.A., Nittrouer, C.A., DeMaster, D.J., Curtin, T.B., 1985. A long, square-barrel gravity corer for sedimentological and geochemical investigation of fine-grained sediments. *Mar. Geol.* 62, 365–370.

Kuehl, S.A., DeMaster, D.J., Nittrouer, C.A., 1986. Nature of sediment accumulation on the Amazon continental shelf. *Cont. Shelf Res.* 6, 209–225.

Kuehl, S.A., Hariu, T.M., Moore, W.S., 1989. Shelf sedimentation off the Ganges-Brahmaputra River system: evidence for sediment bypassing to the Bengal fan. *Geology* 17, 1132–1135.

Kuehl, S.A., Levy, B.M., Moore, W.S., Allison, M.A., 1997. Subaqueous delta of the Ganges-Brahmaputra river system. *Mar. Geol.* 144, 81–96.

Liu, J.P., Kuehl, S.A., Pierce, A., William, J., Harris, C., Aung, D.W., Aye, Y.Y., 2019. The Ayeyarwady and Thanlwin Rivers derived sediments to the Andaman Sea and Bay of Bengal—the geophysical approach. *Mar. Geol.* (to be submitted).

Matamin, Abd, R., Ahmad, F., Mamat, M., Abdullah, K., Harun, S., 2015. Remote sensing of suspended sediment over Gulf of Martaban. *Ekologia* 54.

McKee, B.A., Aller, R.C., Allison, M.A., Bianchi, T.S., Kineke, G.C., 2004. Transport and transformation of dissolved and particulate materials on continental margins influenced by major rivers: benthic boundary layer and seabed processes. *Cont. Shelf Res.* 24, 899–926.

Meybeck, M., Laroche, L., Durr, H.H., Syvitski, J.P.M., 2003. Global variability of daily

total suspended solids and their fluxes in rivers. *Glob. Planet. Chang.* 39, 65–93.

Milliman, J.D., Farnsworth, K.L., 2011. River Discharge to the Coastal Ocean: A Global Synthesis. Cambridge University Press, Cambridge; New York.

Milliman, J.D., Meade, R.H., 1983. World-wide delivery of river sediment to the oceans. *J. Geol.* 91, 1–21.

Milliman, J.D., Syvitski, J.P.M., 1992. Geomorphic/Tectonic Control of Sediment Discharge to the Ocean: the Importance of Small Mountainous Rivers. *J. Geol.* 100, 525–544.

Mitchell, A., Chung, S.-L., Oo, T., Lin, T.-H. & Hung, C.-H. 2012. Zircon U-Pb ages in Myanmar: magmatic-metamorphic events and the closure of a neo-Tethys ocean? *J. Asian Earth Sci.* 56, 1–23 (2012).

Potemra, J.T., Luther, M.E., O'Brien, J.J., 1991. The seasonal circulation of the upper ocean in the Bay of Bengal. *J. Geophys. Res.* 96<sup>https://doi.org/10.1029/91JC01045</sup>. (issn: 0148-0227).

Ramaswamy, V., Rao, P.S. 2014. The Myanmar Continental Shelf. *Continental Shelves of the World: Their Evolution during the Last Glacio-eustatic Cycle*. eds by: Chiocci, F.L.; Chivas, A.R. (Geological Society Memoirs, 41). Geological Society; London; 2014; 231–240.

Ramaswamy, V., Rao, P.S., Rao, K.H., Thwin, S., Rao, N.S., Raiker, V., 2004. Tidal influence on suspended sediment distribution and dispersal in the northern Andaman Sea and Gulf of Martaban. *Mar. Geol.* 208, 33–42.

Ramaswamy, V., Gaye, B., Shirodkar, P.V., Rao, P.S., Chivas, A.R., Wheeler, D., Thwin, S., 2008. Distribution and sources of organic carbon, nitrogen and their isotopic signatures in sediments from the Ayeyarwady (Irrawaddy) continental shelf, northern Andaman Sea. *Mar. Chem.* 111, 137–150.

Rao, P.S., Ramaswamy, V., Thwin, S., 2005. Sediment texture, distribution and transport on the Ayeyarwady continental shelf, Andaman Sea. *Mar. Geol.* 216, 239–247.

Rixen, T., Gaye, B., Emeis, K.-C., Ramaswamy, V., 2019. The ballest effect of lithogenic matter and its influences on the carbon fluxes in the Indian Ocean. *Biogeosciences* 16, 485–503.

Robinson, R. A. J. M. I. Bird, Nay Win Oo, T. B. Hoey, Maung Maung Aye, D. L. Higgitt, X, Lu X, Aung Swe, Tin Tun, Swe Lhaing Win, 2007. The Irrawaddy River Sediment Flux to the Indian Ocean: the Original Nineteenth-Century Data Revisited. *J. Geol.* 115, 629–640.

Robinson, R.A.J., Brezina, C.A., Parrish, R.R., Horstwood, M.S.A., Nay Win, O., Bird, M.I., Myint, T., Walters, A.S., Oliver, G.J.H., Khin, Z., 2014. Large rivers and orogens: the evolution of the Yarlung Tsangpo-Irrawaddy system and the eastern Himalayan syntaxis. *Gondwana Res.* 26, 112–121.

Ross, C.B., Gardner, W.D., Richardson, M.J., Asper, V.L., 2009. Currents and sediment transport in the Mississippi Canyon and effects of Hurricane Georges. *Cont. Shelf Res.* 29, 1384–1396.

Savoye, B., Babonneau, N., Dennielou, B., Bez, M., 2009. Geological overview of the Angola-Congo margin, the Congo deep-sea fan and its submarine valleys. *Deep-Sea Res. II Top. Stud. Oceanogr.* 56, 2169–2182.

Searle, M.P., Morley, C.K., 2011. Tectonic and thermal evolution of Thailand in the regional context of Southeast Asia. In: Ridd, M.F., Barber, A.J., Crow, M.J. (Eds.), *The Geology of Thailand. Geological Society of London Memoir*, London, UK.

Sindhu, B., Suresh, I., Unnikrishnan, A.S., Bhatkar, N.V., Neetu, S., Michael, G.S., 2007. Improved bathymetric datasets for the shallow water regions in the Indian Ocean. *Earth Syst. Sci.* 116, 261–274.

Syvitski, J.P.M., Saito, Y., 2007. Morphodynamics of deltas under the influence of humans. *Glob. Planet. Chang.* 57, 261–282.

Syvitski, J.P.M., Kettner, A.J., Overeem, I., Hutton, E.W.H., Hannon, M.T., Brakenridge, G.R., Day, J., Vorusmarty, C., Saito, Y., Giosan, L., Nicholls, R.J., 2009. Sinking deltas due to human activities. *Nat. Geosci.* 2, 681–686.

Tolman, H.L., Balasubramanyan, B., Burroughs, L.D., Lawrence, D., Chalikov, D.V., et al., 2002. Development and implementation of wind-generated ocean surface wave models at NCEP. *Weather Forecast.* 17, 311–333.

Vigny, C., Socquet, A., Rangin, C., Chamot-Rooke, N., Pubellier, M., Bouin, M.-N., Bertrand, G., Becker, M., 2003. Present-day crustal deformation around the Sagaing fault, Myanmar. *J. Geophys. Res.* 108. <sup>https://doi.org/10.1029/2002JB001999</sup>.

Winterwerp, J.C., de Graaff, R.F., Groeneweg, J., Luijendijk, A.P., 2007. Modelling of wave damping at Guyana mud coast. *Coast. Eng.* 54, 249–261.

Wyrtski, K., 1973. Physical oceanography of the Indian Ocean. In: Zeitschel, B., Gerlach, S.A. (Eds.), *The Biology of the Indian Ocean*. Springer Verlag, Berlin, pp. 18–36.